MRS ◖Communications

Early Career Materials Researcher Prospective

Current trends in macromolecular synthesis of inorganic nanoparticles

Brendan Karafinski, and Nairiti Sinha, Department of Materials Science and Engineering, Pennsylvania State University, University Park, PA 16802, USA

Address all correspondence to Nairiti Sinha at **njs6356@psu.edu**

Abstract

Inorganic nanoparticles are a critical component in a broad range of applications spanning catalysis, sensing, optics, and electronics. The nucleation and growth mechanisms involved during their synthesis are known to be crucial for controlling their final performance. Macromolecules can display sequence definition, inherent chirality, metal ion targeting moieties, and can also form self-assemblies, affording them the ability to not only stabilize but also precisely control the synthesis and organization of nanoparticles for an intended application. Herein, we report the recent trends in inorganic nanoparticle synthesis mediated by peptides, peptoids, DNA, other biopolymers, and synthetic polymers. Important design parameters and future trends are also discussed.

Introduction

Inorganic nanoparticles have had a resurgence in interest over the past decade due to exhibiting unique properties as compared to their bulk counterpart. Their large surface area, surface plasmon resonance,[1] and biocompatibility have been the primary properties contributing to their vast use in catalysis, biosensing, and pharmaceuticals. Catalysis takes advantage of their high surface area and surface reactivity to induce oxidation and hydrogenation. For example, gold nanoparticles have been utilized as a catalyst in the reduction of 4-nitrophenol,[2–6] a common pollutant. To be an effective catalyst, the nanoparticles must remain small and avoid agglomeration. Commonly, catalytic nanoparticles are attempted to be stabilized via biological capping agents,[2,3,6] while others embed the nanoparticles in a membrane[4,7,8] or framework.[5,9] Meanwhile, biosensors are evolving by enhancing their light absorption and scattering by implementation of inorganic nanoparticles and tuning their plasmonic properties. When irradiated with light, the surface electrons (plasmons) oscillate and change the local refractive index of the environment, which can be measured in real time. The presence of noble metal nanoparticle plasmons greatly increases the signal detection capabilities, allowing for early screening of cancers[10–13] as well as other molecule monitoring.[7,14–17] In contrast, pharmaceuticals are exploring inorganic nanoparticles for different therapeutic options, such as target drug delivery and photothermal therapy. For example, gold nanoparticles are biocompatible and can be decorated with different biopolymers that can help direct the particles to target places within the body. Additionally, these biopolymers can also be bound to drugs which can then be directed to their intended destination and released.[18–20] Photothermal therapy aligns itself with targeted drug delivery, except the nanoparticle itself is the treatment.

While inorganic nanoparticles have found themselves in the spotlight once again, their properties are synthesis dependent.

Traditionally, techniques can be categorized as either top-down or bottom-up for synthesizing inorganic nanoparticles. The top-down approach most generally involves reducing the size of bulk materials, such as metals, to micron and in some instances, sub-micron particles. Recently, improvements have been made in various top-down techniques. Pulsed laser ablation, for example, allows for some control over the resulting particles due to the ability to adjust laser parameters, aqueous media, and ablation time; however, the reported micrographs have clear agglomeration and exhibit polydispersity.[21,22] Ball milling comes with other less appealing disadvantages including high energy consumption, long milling times, and product contamination.[23] Evaporation–condensation techniques are also costly due to the vaporization of metal precursor materials, but they do offer a unique alloyed particle, [24] similar to that of some laser-ablated particles.[25]

In contrast to the aforementioned typical top-down methods, bottom-up synthetic techniques offer several advantages, the most notable one being the biomimetic and sustainable synthesis of organic–inorganic and hybrid nanoparticles under mild solution conditions that also display complex shapes and tunable sizes.[26] Specifically, macromolecules that are used during synthesis can impose chirality in the resulting inorganic nanoparticles, which has a substantial impact on the optical properties and design considerations for biosensors.[27] Furthermore, nanoparticles synthesized using macromolecules show superior surface passivation which is crucial for all applications. Additionally, for photothermal therapy and drug delivery applications, such macromolecules can be further bound to a site-directing biopolymers and then irradiated causing rapid heating of the particle which will result in cancer cell death.[7,28,29]

Motivated by aforementioned developments, innovation in macromolecule-assisted synthesis methods is being actively

pursued to improve the process-property-performance attributes of resulting nanoparticles, especially as the macromolecules themselves become more sophisticated.

The traditional mechanism for NP formation is a thermodynamic process called crystallization, which includes a growth[30] and nucleation[31,32] step. Various molecules present in a system can function in one or numerous roles such as a templating, reducing, or capping agent all impacting the overall thermodynamics. It is important to note that each class of macromolecule differ in the role in which they play during crystallization based on the complexity of their structure or lack thereof. The technical aspect of how the various molecules participate in crystallization will not be covered in the below sections as it is outside of the scope of this paper.

This perspective article highlights the most relevant design considerations pertaining to peptides, peptoids, DNA, other biopolymers, and polymers for a targeted application of the resulting nanoparticle (see Fig. 1). The most current research within each class of macromolecules is presented in the latter sections. Additionally, some innovative trends are also highlighted in the last section followed by a perspective in the future outlook section. The findings of relevant papers are summarized in Table I. The authors note that this article is not meant to be an exhaustive review of the fundamentals of macromolecule-mediated inorganic nanoparticle synthesis, rather we aim to provide a starting point for the reader and present the most recent and impactful papers in the last five years. Exhaustive reviews for each macromolecular type are indicated in every section.
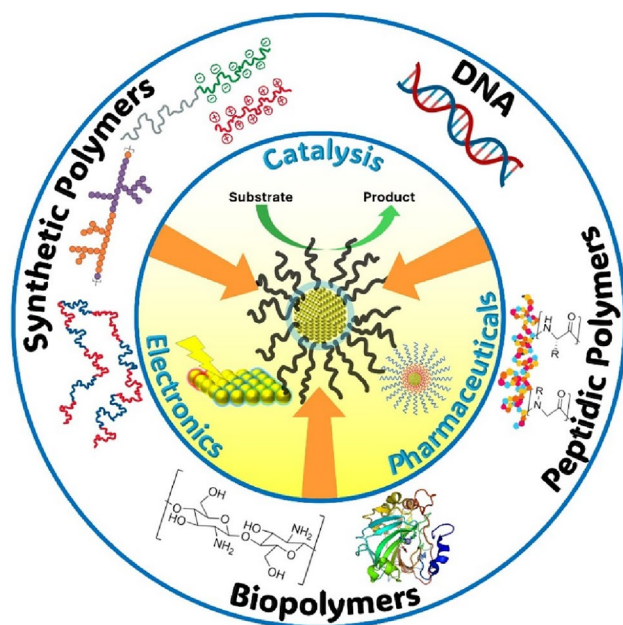
Figure 1. Illustration of macromolecular synthesis of inorganic nanoparticles and their various applications. Different classes of macromolecules that are used for nanoparticle synthesis and templating are listed in the outer ring and major applications that utilize the resulting nanoparticles are shown in the inner ring.

Bottom-up synthesis of inorganic NPs
Peptides

Peptides are sequence-defined biomacromolecules of amino acids and are short domains of structure within proteins. Peptides are commonly used in the bottom-up approach due to their ability to reduce and cap inorganic nanoparticles. The versatility of peptides is that there are twenty proteogenic amino acids that can be sequenced to make a peptide that has unique properties tailored to produce a desired nanoparticle for a specific application. For this type of macromolecule, a major design consideration is the fact that peptides are chiral, and this property can lead to handedness wherein the peptide-binding orientation will be reflected in the resulting nanoparticle morphology. It is important to understand chirality because of the enantioselectivity that is observed in many biochemical reactions,[33] and because of the recent development of chiral meta-materials with exceptional light-manipulating capabilities, such as polarization control, a negative refractive index, and chiral sensing.[34] Besides peptide chirality, environmental factors, and material selection play a role in the resulting morphology of inorganic NPs. We direct the reader to Pazos and co-workers[35] for an exhaustive discussion on this topic.

Recently, Nam et al. have synthesized large-scale chiral AuNPs that have strong chiral optical properties. These NPs can have their handedness and chirality flipped by substituting the other enantiomer during synthesis.[36] This feat has also been demonstrated by He and colleagues with an illustration of their system in Fig. 2(a).[37] The electron micrographs below [Fig. 2(b)] show the difference in morphology when the enantiomer of ferrocene−diphenylalanine peptide is changed during synthesis. These morphological changes are accompanied by a complete reversal in the chiroptic properties measured in the circular dichroism measurements as shown in Fig. 2(c). Being able to control the handedness of NPs will help improve the understanding of enantioselectivity and how crystalline surfaces adsorb differently with the same molecules, as well as pave the way for advancing chiroptic applications. In another study, Slocik et al. reported the chiral restructuring of a peptide enantiomer when bound to AuNP surfaces.[38] Rather than the different enantiomer peptides during synthesis leading to a NP with reversed chirality, the same peptide could exhibit circular dichroism (CD) spectra of either type, depending on whether the peptide was bound to the gold surface. The applicability of this feature may be neurotoxin or venom treatment, but this cannot be fully realized until computational models can better explain the mechanism behind this phenomenon.

In most cases, the addition of heat to a system improves the reaction kinetics and is needed to drive electron transfer between reducing side groups and metal ions in solution. This, however, is a well-debated source of polydispersity throughout the nanoparticle (NP) community. At an attempt to circumvent inhomogeneous heating, Mukha and company

Table I. Summary of macromolecule type, species involved and characteristics, and applications of resulting nanoparticles.

Macromolecule class	Specific material	Templating agent/Stabilizer	Reducing agent	Nanoparticle Species	Shape	Application	Features	Ref
Peptide	poly(ethylene oxide)-b-poly(l-histidine)-b-poly(γ-benzyl-l-glutamate)	poly(l-histidine)	poly(l-histidine)	Au	sphere	Photothermal therapy	First reports of NP synthesis via peptides in the absence of reducing agent	28
Peptide	cysteine / cysteine peptides	cysteine	cetyltrimethylammonium bromide (CTAB) / Ascorbic acid	Au	cubic / helicoid	3D chiral nanostructures for plasmonic meta-materials	Requires AuNP seeds in order to template 3D nanostructures	36
Peptide	l-FlgA3 (DYKDDDDK-PAYSSGAPPMPPF) / d-FlgA3 (DYKDDDD-KPAYSSGAPPMPPF)	l-FlgA3 / d-FlgA3	HEPES / NaBH4	Au / Pd	sphere / nanorod	controllable catalytic activity of 4-nitro-phenol	Peptide enantiomer directly templates chiral motifs onto NPs	38
Peptoid	Nce8Nab4Ndc4	Ndc and Nab residues	N/A	Au / Pt / Pd	coral	enhanced plasmonic responses / distinct catalytic properties	Used only as a templating method for synthesis of nanostructures	48
Peptoid	Car9-sfGFP(G51C)-A3	Car9/A3	citrate / HEPES / TEAA	TiO_2 / Au	nanocomposite	photocatalyst for organic dyes	Nucleation and growth of different NPs onto the protein-peptoid hybrid nanostructure	55
DNA	DNA origami	DNA	tetraethyl orthosilicate (TEOS) / trimethoxysilylpropyl-N,N,N-trimethylammonium-chloride (TMAPS) / temperature	SiO_2	various nanostructures	biosensing and nano-electronics	A regulated Stöber reaction can be used to design origami templates with specifically located silica-binding strands	56
DNA	DNA sodium salt from herring testes	DNA	temperature	Bi_2MoO_6	nanoplates	supercapacitors	This provides a simple and low-cost method for producing high-performance supercapacitor electrode materials	57
Other biopolymers	R5CsgACBD / chitin	sugar / R5CsgACBD / chitin	Ti (IV) bis-(ammonium lactato)-dihydroxide (TiBALDH)	SiO_2 / TiO_2 / Ga2O3	3D porous structures	artificial photosynthesis	Sugar cubes acting as a scaffold for self-assembled porous metal nano-hybrids	67
Other biopolymers	Silk fibroin (GAGVGY-GAGVGAGYGAGYG AGAGAGY)	silk fibroin	silk fibroin	Au	single crystal	catalysis	Silk fibroin's unique sequence optimally nucleates gold and promotes large 2D single crystals	71
Polymer	polystyrene-block-poly(4-vinylpyridine)	polystyrene-block-poly(4-vinylpyridine)	N/A	AuNPs / CdSe QDs / ZnS QDs	onion-like layered particles	bioimaging and diagnostics	Highly engineered method for creating solvent sensitive fluorescently switchable layered NPs	84
Polymer	sugar-based comb-like polyurethanes	sugar-based comb-like polyurethanes	borohydride	Au	spherical	printable nanocomposite inks	Comb-like polyurethanes act as an encapsulating agent for Au	94
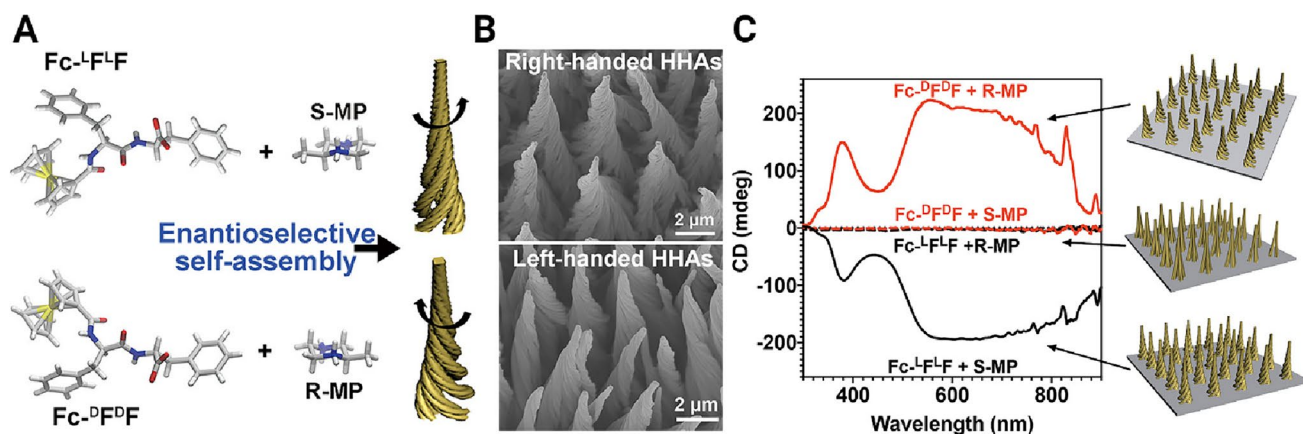
Figure 2. (a) Illustration of ferrocene–diphenylalanine peptide enantiomers and resulting morphologies, (b) SEM, and (c) CD spectra of corresponding morphologies. Adapted from the abstract and Fig. 3 in Wang.[37] Copyright © 2021 American Chemical Society.

used photoactivated tryptophan to drive nucleation.[39] Successful implementation of this technique has been demonstrated by the change in the LSPR-band between samples that were irradiated and the ones that did not, showing three times increase in gold nanoparticle (AuNP) formation. Not only were more AuNPs synthesized, but peak narrowing of UV–VIS data suggests lower particle size distribution, which is an attractive characteristic for catalysis and biosensing. Besides temperature, pH is another environmental factor that can be controlled and may influence NP formation.

Experiments conducted by Baez-Cruz et al. demonstrated pH being a knob that can be used to control NP morphology.[40] By examining their anionic and zwitterionic *L*-Arginine-derived system with Raman scattering and molecular dynamic simulations, they were able to suggest an underlying mechanism that controls the morphology. They postulated that as the pH is increased, there is an increase in the amines preferential adsorption over ammonium groups, changing the resulting morphology. Another development in peptide-mediated NP synthesis has been by Feng et al. and their work with Amyloid β ($A\beta_{25-35}$) peptides.[41] They uncovered that by changing the incubation time in their phosphate buffer, $A\beta_{25-35}$ would assemble different templates. They could make nanoparticles, nanoribbons, nanofibrils, and nanoflowers. This is noteworthy because catalytic properties are governed by reactive surfaces and each morphology will come with an associated enhancement to a specific catalytic application, which was observed by the reduction of 4-nitrophenol. Chiral NPs are not only being implemented as powerful tools for biosensing and catalysis but are also being investigated for antibiotic applications since a lot of bodily functions are enantioselective. Chen et al. have reported that spiked chiral AuNPs synthesized by Cysteine and Phenylalanine dimer-mediated growth of bipyramidal seeds showed chirality-dependent antibacterial properties.[42]

Peptides have shown their ability to nucleate and assemble inorganic nanoparticles for various applications. Their strength comes from their ability to be sequentially defined, allowing for intricate structures and assemblies to be made that can both

nucleate and bind to different inorganic materials. Pozzo and co-workers recently published a paper reporting how AuNP morphology changed as Au binding peptides were modified in 64 different reaction conditions to span a large amount of the design space.[43] To compliment that, Figat et al. reported how the twenty different naturally occurring amino acids (constituent parts of a peptide) both bind and reduce gold in solution.[44] Regarding other reaction parameters, Knecht and company reported how the same peptide with different strength reducing agents impacts the resulting morphology.[45] To understand how the amino acid sequence impacts gold binding, Janairo published a meta-analysis reporting the sequence rules that impact such property and suggested specific positions within the sequence have a larger impact than others, and tryptophan and arginine are important amino acids to consider.[46] Further examination of the peptides that have demonstrated their ability to reduce or template different metallic ions suggest a few different functional groups to be further investigated. For example, phenylalanine, tryptophan, and tyrosine are common amino acid species present in most peptide sequences. This suggests that there must be something related to the presence of their benzene, indole ring, and phenyl groups that may be stabilizing the different ions allowing for templating or reduction.

Peptoids

Another macromolecule type with many of the same benefits as peptides is peptoids. Both peptides and peptoids can be sequentially defined to impact their ability to synthesize and template inorganic NPs. Peptoids are peptide-mimetic but are achiral because the side-chain functionality is on the nitrogen rather than the α-carbon that results in lack of backbone hydrogen bonding. More extensive detail on peptoids can be found in the review by Chen et al.[47,48]

Chen et al. have utilized peptoids[49] that contain analogues of common hydrophilic and hydrophobic amino acids. By doing so, their team has developed a built a fundamental understanding of these peptoids. Specifically, they have reported a

"rule of thumb" for templating Au coral particles which states that such particles form in the presence of amino-containing group, requires strong side-chain hydrophobicity and a precise arrangement of peptoids during the growth phase. These coral-shaped AuNPs offer unique plasmonic enhancements which would find use in biosensors.

Merrill et al. conducted a similar peptoid sequence study but instead of investigating self-assembly and AuNPs synthesis, they opted to try and tune catalytic properties of palladium nanoparticles (PdNPs).[50] By systematically changing the peptoid assemblies, they were able to produce 1D fibers and 2D membranes in which the assembly of PdNPs differed, exposing different facets and thus changing the catalytic properties of the overall assembly. CdSe quantum dots have also been shown to template on peptoid tubes and sheets via covalent linkage.[51] Likewise, enhancements in plasmonic properties have been realized in similar coral AuNPs.[52] Mechanical property enhancements of hydrogels have also been looked at with applications in tissue engineering.[53] Further understanding on how the peptoid sequence is employed to tune inorganic crystallization can be found in Yang and colleagues in depth review.[47] Peptoid sequence has also been used to stabilize different facets leading to control over resulting NP morphology. By manipulating the sequence, different crystal facets of Au were stabilized leading to the preferential growth of fivefold-twinned nanostars[54] which typically are formed from seed-mediated growth.

Recently, a controlled mineralization of anatase crystals and gold NPs was demonstrated through protein-modified peptoid nanotubes. With these hybrid structures, Ma et al. were able to synthesize monodisperse anatase (TiO$_2$) nanocrystals on the order of sub-5-nm regime with the ability to narrowly control size by changing protein surface density, identity and valence of surface-binding peptides, and mineralization time.[55] This setup was also used to synthesize monodisperse AuNPs. Additionally, they were able to build a bifunctional mineralizing peptoid-protein construct with the mechanism as shown in Fig. 3(a) that has both a titania and gold binding sites which led to the successful development of TiO$_2$/Au nanocomposites. The structure is shown in Fig. 3(b,c) with scanning electron microscopy (SEM) and transmission electron microscopy (TEM) images of the co-templated TiO$_2$/Au nanocomposite and characterization in Fig. 3(d,e) showing the atomic structure and corresponding lattice spacing and diffraction peaks confirming both exist. All the NPs that were synthesized on these scaffolds were under 4 nm and stable which is something that has not been seen previously in other biomimetic mineralization routes. An application of interest that Ma et al. has identified these constructs can be tuned for is photocatalytic degradation of organic dyes.

DNA

DNA has recently been a very popular tool used for site-specific fabrication of different materials. One such case has been method for making silica nanostructures[56] by Ding and co-workers. They were able to make such nanostructures with such precision by utilizing a protruding dsDNA strand which served as the nucleation point during silicification, which should sound like the protein-modified peptoid nanotubes mentioned previously. This technique could be pivotal in creating layered dielectrics for various electronic applications.
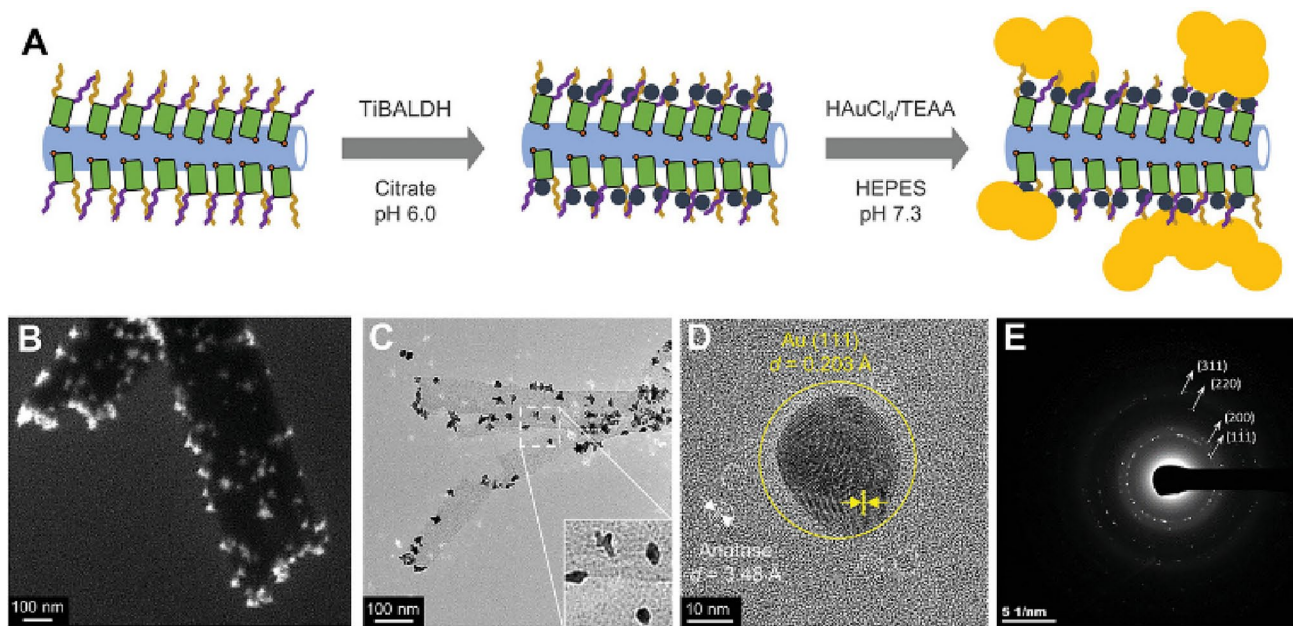
Figure 3. (a) Illustration of sequential mineralization of TiO$_2$ and Au onto protein-modified peptoid nanotubes. (b) SEM, (c) TEM, (d) HR-TEM, and (e) Selected area diffraction pattern of the TiO$_2$/Au-mineralized peptoid nanotubes. Adapted from Fig. 5 in Ma.[55] Copyright © 2022 Wiley-VCH GmbHDNA.

A low-cost and effective alternative to traditionally grown Bi_2MoO_6 nanoplates for electrode materials has recently been demonstrated with DNA templating.[57] By varying the concentration of the DNA during the synthesis step, the diameter and thickness could be shifted to larger or smaller plates on the order of 30-180 nm. The apparent mechanism seems to be that the dissolved DNA formed micelles on other DNA segments, and the negative charge would attract the positive Bi ion and allow nucleation and growth on the surface via electrostatic interactions.

Improvements to the structural stability of DNA-Chitosan hydrogels have been realized by charging polysaccharides in a DNA solution. By doing so, both constituents have aromatic and nitrogen-containing groups which make this hydrogel a multitarget absorbent for metal ions. This leads to the entrapment of ions within the hydrogel and NP reduction onto the scaffold. Morikawa et al. have successfully used this technique to synthesize 2–3-nm AuNPs, producing a metallic hydrogel with catalytic activity.[58]

Combining the idea of functionalized NPs with DNA origami constructs, Mathur et al. fabricated precisely placed gold nanorods (AuNRs) into plasmonic coupling regimes to control red and blue shifting of LSPR peaks.[59] By coating AuNRs with binding DNA strips, they were able to attach these functionalized particles to DNA triangles that had DNA-binding sites which the AuNRs could then attach to. This goal was accomplished with 20 nm × 50 nm and 10 nm × 90 nm AuNRs to make numerous shapes successfully. A similar concept was also used by Liu et al. to make 2D chiral plasmonic superstructures which they programmed the chiral motif by the number of AuNR pairs, and the size of the AuNRs by the underlying DNA template.[60] In Fig. 4(a), a schematic demonstrates an example of the self-assembly of the DNA triangles into the different hexamers. Atomic force microscopy (AFM) was provided in Fig. 4(b,c) of both showing the size of the structures. The different hexamers can be made to be chiral or not depending on the triangular template used depicted in Fig. 4(d–i) SEM images. More work has been done in further understanding site-specific polynucleotide brushes which influences the silicification process, as well as changing the molecular characteristics of the DNA to deter aggregation.[61]

DNA templating and functionalization has also led to the development of Bi_2S_3 NPs that can accumulate in the infarcted area allowing for improved photoacoustic imaging of myocardial infarction.[62] Zhou et al. have also developed a DNA-Mn nanoflower hybrid using the synergistic effects tumor site targeting and cellular uptake from the DNA and Mn for enhanced MRI signal enhancement.[63] Similarly, a glyphosate (GLYP) biosensing system has been developed with DNA-templated
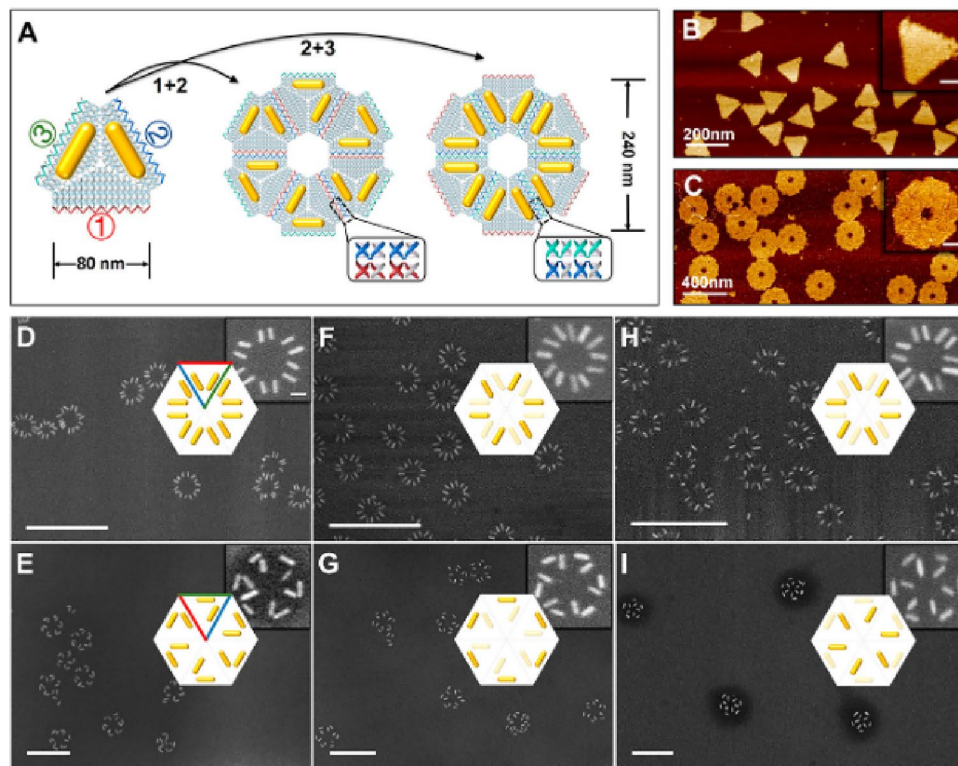
Figure 4. (a) Schematic of self-assembly AuNRs on DNA triangles, (b, c) AFM of DNA triangles and hexamers. The scale bar for the zoom in the range of (b) is 40 nm and 80 nm in c. (d-i) SEM images of bi-stars and pinwheels of AuNR assemblies. The colored edges in (d, e) are consistent with that in (a) showing how they were assembled. The scale bars for the zoomed-out SEM images is 400 nm and the zoomed-in is 50 nm. Reprinted from Fig. 2 in Liu.[60] Copyright © 2021 American Chemical Society.

copper NPs with high selectivity and fast testing speeds. The presence of GLYP chelates Cu ions preventing the reduction of copper NPs on the DNA scaffold, therefore preventing the formation of fluorescence peaks and therefore indicated that GLYP is present in the system.[64]

Other biopolymers

The area of inorganic NP synthesis and templating using biopolymers such as sugars and proteins are aimed at "green synthesis" of popular inorganic NPs. There are numerous exotic biopolymers that have found success in either reducing precursors or capping and stabilizing NPs. The most recent and compelling publications have been included in this section. More can be found in a more comprehensive review Jesionowski and colleagues.[65] It should be mentioned here that a major field of biopolymer mediated synthesis is in the biomineralization of other inorganic materials such calcium containing carbonates and phosphates which we have not discussed here. For completeness, we direct the reader to a recently published report from Keating that includes recent innovation in novel micro-reactors that utilize liquid–liquid-phase coexistence as a mechanism to control reaction environments and thus impact the resulting mineralization of such calcium carbonates and phosphates during the biomineralization process.[66]

Li et al. genetically modified a self-assembly capable structural amyloid protein with a SiO_2 nucleation peptide.[67] By doing so, they were seemingly able to guide nucleation of SiO_2 NPs via modified amyloid fibers, where non-modified proteins did not promote the deposition of SiO_2 NPs. Something else they were able to accomplish was fabricating self-supporting modified protein-chitin complex scaffold for TiO_2 mineralization with a sugar cube as a bulk template as depicted in Fig. 5(a). The sugar cube in Fig. 5(b) was submerged in an ink containing this protein-chitin complex and cured, triggering reassembly of the amyloid nanofibers throughout the whole matrix of the sugar cube [Fig. 5(c)]. Finally, this sugar cube was dissolved and what remained was a high surface area porous template. This template was then submerged in a buffered aqueous solution with different metal ions that mineralized on the surface. In Fig. 5(d,e), scanning electron microscopy-energy-dispersive spectroscopy (SEM–EDS) and scanning transmission electron microscopy (STEM–EDS) analysis indicate the presence of Ti, Ga, and Si successfully mineralized on the surface. Their future work states that this could hypothetically be used to construct an artificial photosynthesis system where the TiO_2 acts as a light antenna providing electrons to an engineered *Escherichia coli* strain that has a hydrogenase gene cluster, thus synthesizing hydrogen.

Small biopolymers are often employed to stabilize NPs during synthesis. In the case of $CaSO_4$, 58-nm NPs were synthesized by co-precipitation but using gelatin as a green stabilizer.[68] Since these NPs are capped with a biopolymer, they can find themselves in a variety of pharmaceutical applications, such as biocatalyst.

Advances in alternative and green methods for synthesizing NPs have been demonstrated recently. For instance, marine bacterial exo-polymers were used as alternative reducing agents for noble metal NP synthesis. Three exopolysaccharides were produced from bacteria from shallow hydrothermal vents and successfully nucleation Ag/AgCl/Au NPs as well as stabilization.[69] Enzymes have also been recently reported to have been used in the green synthesis of inorganic NPs. Three oxidoreductive enzymes were discovered to successfully act as a bioreductant of AuNPs in the presence of different carbohydrates which changed the resulting NP size and shape.[70] Notably, massive 2D Au single crystals have been successfully synthesized by Lv et al. in which millimeter length crystals have been achieved[71] which are highly desirable for catalytic applications and single-molecule sensing. It was reported that silk fibroin has a specific amino acid sequence that synergistically with chlorine can enable conditions in which kinetically controlled synthesis of single crystal Au atomically smooth surfaces can be synthesized.

Another common macromolecule that has been used for inorganic nanoparticle scaffolding and assembly is cellulose. Oxidized bacteria cellulose nanofibers were used to template gold by Thoidi et al. with the intention of being used as an injectable biomaterial for cardiac tissue regeneration.[72] AuNPs were also successfully made with carboxy methyl cellulose (CMC) which were able to be made between 10–90 nm by Doghish et al.[73] These CMC-AuNPs were shown to be effective, anti-cancer, antifungal, and antimicrobial with the mechanism suggested to be related to the activation of necrosis and apoptosis. Gold was also templated onto cationic cellulose nanofibrils by Alle et al. in the form of a film that was shown to be recycled up to five times as a glucose detection without decrease in efficacy.[74]

Copper oxide NPs were synthesized on electrospun cellulose nanofibers by Haider et al.[75] These NPs were 3 and 7 nm in size, and the antibacterial properties shown promise against gram-negative bacteria. The CuO NP-coated cellulose demonstrated the CuO to be responsible for the antibacterial response and are expected to make useful wound dressing materials. CuO NPs have also been synthesized by Mathew and company, but with nanocellulose films with targeted application in water purification.[76] It was reported that these hybrid films can likely be used as a universal substrate for the nucleation of many different heavy metal ions and can be upcycled which makes for a sustainable source of material. Similarly, Danish and company used cellulose polymer paper as a scaffold for AgNPs to enable a highly porous structure with high surface area that can be decorated with silver to promote catalytic activity toward common water pollutants.[77] Magnetic NPs ranging from 6 to 14 nm have also been selectively precipitated onto bacterial cellulose and have been reported to selectively filter antimony from aqueous solution.[78]

Hydroxyethyl cellulose (HEC) nanostructures were used as a template for synthesizing Ag, Au, and Au/Ag-alloyed
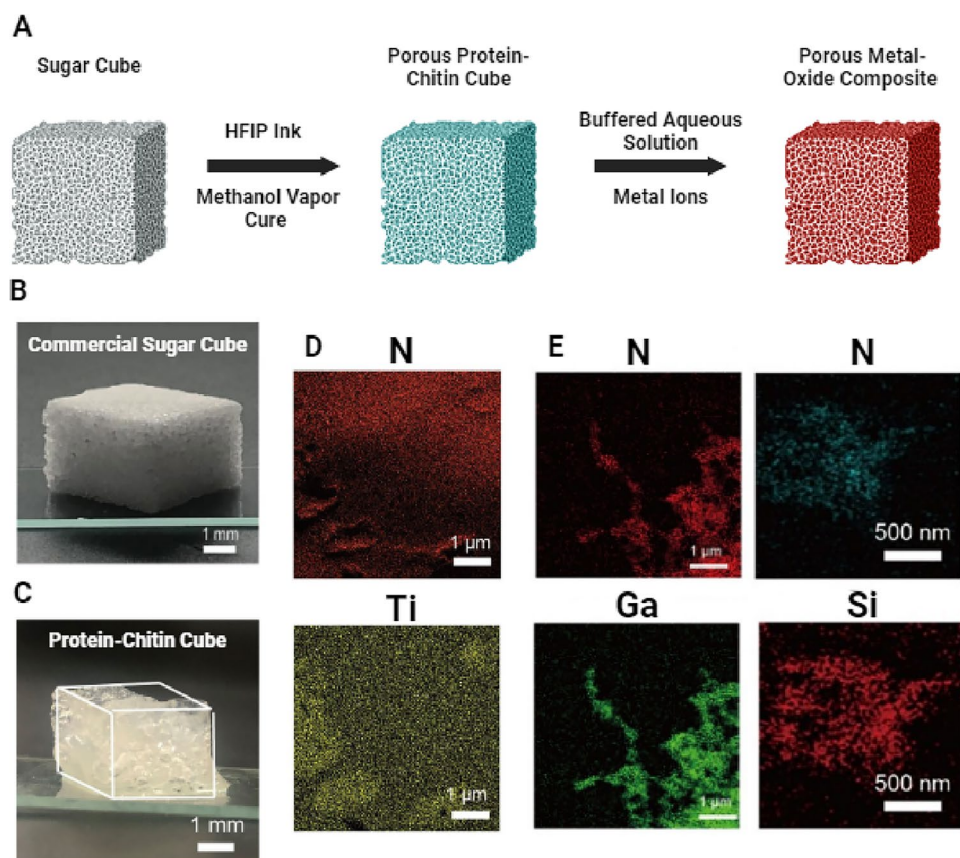
Figure 5. (a) Illustration of how porous metal oxide composites are fabricated from coating sugar cubes with protein-chitin complex that promote mineralization at the surface, (b) commercial sugar cube scaffold, and (c) resulting protein-chitin cube following the ink soak and cure. (d) SEM–EDS demonstrates the ability of protein modification to promote mineralization of Ti and (e) STEM-EDS of Ga and Si on the surface. Adapted from Figs. 4, S2, and S12, S16 in Li.[67] Copyright © 2020, © The Author(s) 2020.

NPs. Ahmed et al. used the HEC macromolecules as a green alternative scaffold for making such NPs and reported that the Au/Ag alloy had superior antipathogenic actions than either Ag or Au individually.[79] This technique can likely be employed to synthesize other unique alloyed NPs for many different applications. Another, different version 2,2,6,6-tetramethylpiperidine-1-oxyl (TEMPO)-cellulose nanofibrils were used as a one-pot method for reducing AgNPs. By doing so, this system can be leveraged as a cysteine detector, where upon cysteine–AgNP interactions, the surface plasmon resonance changes, and the solution changes colors dramatically.[80]

Polymers

Synthetic polymers and polyelectrolytes have been widely employed as ligands during NP synthesis. By complexing achiral amphiphilic diblock copolymers poly(styrene-block-4-vinylpyridine) (PS-b-P4VP) with R/S-mandelic acid (a chiral dopant) and using steric hindrance to their advantage, Kim et al. have successfully synthesized chiral metal oxide NPs.[81] The steric hindrance within the inverse micelle inhibits the racemization of the R/S-mandelic acid core, imparting chirality to subsequent NPs formed via hierarchical chirality transfer. They showed that magneto-chiroptic properties can be tuned by controlling the direction of the external magnetic field for paramagnetic NPs.

Using PS-b-P4VP and polystyrene-block-poly(methyl methacrylate) (PS-b-PMMA) and meticulously post-processing, block copolymer (BCP) NPs were able to be used as templates for metal oxide NPs. Weisbord et al. were able to construct BCP NPs with control over size distribution, degree of phase separation which varied the internal structure, and porosity which can be altered for application specificity.[82] With these, they utilized sequential infiltration synthesis, which exposes the different PV4P and PMMA domains to gas-phase metal–organic precursors which selectively deposit onto each, respectively, to successfully synthesize hybrid organic–inorganic composites. This technique expands the materials that can be templated, as well as allowing for exotic morphologies to be analyzed. Other BCPs have been demonstrated as effective gold-decorated porous membrane for catalytic flow reactors to transform nitrophenol to aminophenol.[83]

Such BCP systems have also found applications in bioimaging, sensing, and diagnostics due to their ability to be fluorescently switchable in some instances. Kim and co-workers developed a doubly alternate-layered NP array that has alternating AuNPs and CdSe/ZnS QDs in which these particles exist in different layers.[84] Figure 6(a,c) shows TEM images of the as-produced PS-b-P4VP BCP NPs with the PV4P domain being stained with a contrast agent to help demonstrate the nano-sized layering. The AuNPs and CdSe/ZnS NPs appear as dark spots in the TEM images in Fig. 6(b,d) of the cross-sectioned BCP NP to get a better look at the internal structure. Upon solvent-selective swelling of layers, NP-QD distances can be large, and fluorescence is "on" by preventing non-radiative energy exchange between the NPs and QDs or in the absence of swelling BCP can be fluorescently "off." Jia et al. have developed aromatic block copolymers that can be self-assembled into micro-reactors for sub-micron cube like AgNPs as building blocks for SERS nanosensors.[85]

An innovative cancer therapy has been fabricated by Alle et al. in which pH sensitive AuNPs were decorated with doxorubicin-xanthan gum and will preferentially release the drug at the tumor site.[86] Rai et al. repurposed Soloplus, a commercial graft copolymer, to develop dequenched Ag/Au hybrid NPs for advancements in biophysical chemical sensor development.[87] By modifying the ratios of gold to silver ions in solution with Soloplus, the resulting optical properties can be altered upon exposure to UV light. He et al. used polyhexamethylene biguanide (PHMB) to template AuNPs to induce a synergistic effect between the PHMB antimicrobial properties and the gold photothermal effect.[88]

Synthesizing atomically precise inorganic NPs with strict size and shape control and good fidelity has been accomplished by Liu et al. in their synthetic polymer brush system.[89] Using light-mediated surface-initiated atom transfer radical polymerization methods, they prepared an atomically precise brush polymer-functionalized silicon wafer. When exposed to inorganic precursor solution, the resulting NP was 78 ± 7 nm thick when using a template of 75 ± 6 nm. Jin and company were able to generate sub-5-nm AuNPs using loop-cluster coronas that were dispersed on the surface of a polymer vesicle.[90] They were able to avoid agglomeration of the AuNPs as they reduced by having them compartmentalized throughout the loop clusters. The benefit of this method is that by changing the loop size, the AuNP size can be changed which will impact the subsequent catalytic properties of the vesicles.

Importantly, Bressan et al. have fabricated a new microfluidic device that utilized fused deposition modeling for the purpose of synthesizing inorganic NPs. They reported that the device was able to synthesize both Ag and Au NPs. The resulting Ag and Au NPs were 5–8 nm and 20–34 nm, respectively, and both were shown to be stable for 3 week.[91] With relation to additive manufacturing, Saggiomo and co-workers demonstrated the ability to embed AuNPs in a 3D-printable ink yielding the ability to manufacture a dichroic nanocomposite.[92] By a modified Turkevich method, the AuNPs that were produced possessed dichroic properties which they then capped with polyvinyl acid, a known capping agent, and common 3D printing material. The printability nor the mechanical properties were drastically influenced by the presence of AuNPs in filament. Similarly, Estrada and co-workers used polyvinylpyrrolidone (PVP)-capped AuNPs as a printable ink for wearable electronics.[93] The PVP is well studied and allows for precise control over the AuNPs size and shape, while also being chosen for its good adhesion properties to many different substrates.

Other advancements in 3D-printable nanocomposites include the combination of both organic and inorganic components to the print feedstock material. For example, carbohydrate-modified polyurethanes have been shown to adequately template AuNPs and alter rheological properties allowing for them to be 3D printed.[94] Using click chemistry, the carbohydrate was added to the urethane chain, allowing for control over how substituted the polymer became, giving the ability to tune the physicochemical properties as a nanocomposite. Similar work has recently been published by Loughney and co-workers where they replaced the traditional capping agent in a pre-ceramic with poly(pyridylmercaptopropyl)methylsiloxane (PyMPS), to act as the capping ligand, reducing agent, and reactant allowing for the creation of a printable and tunable
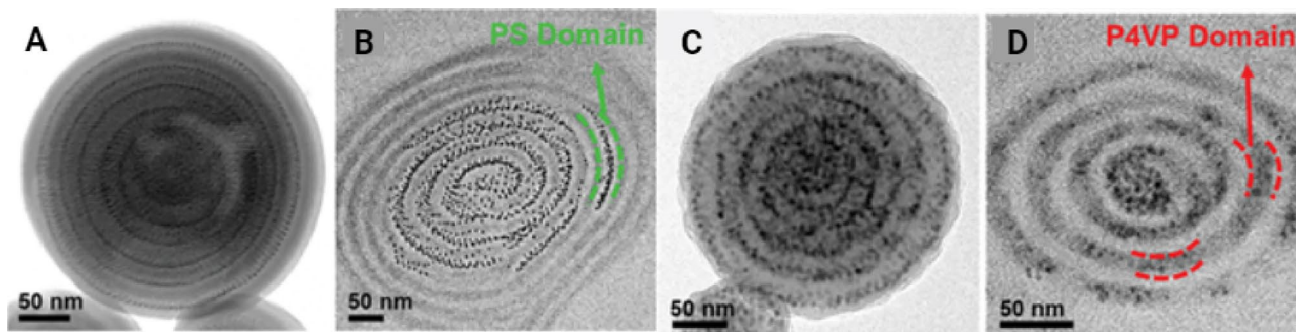
Figure 6. TEM images of (a) the as-produced and (b) the cross-sectioned PS10k-b-P4VP10k microspheres with Au@PS NPs (Au-BCP), and (c) the as-produced and (d) the cross-sectioned PS10k-b-P4VP10k particles with CdSe/ZnS QDs (QD–BCP). The P4VP domains were stained with iodine vapor to enhance their contrast in the TEM images. Adapted from Fig. 1 in Kim.[84] © 2021 Wiley-VCH GmbH.

copper sulfide nanocomposite.[95] More can be found on recent trends of polymer that mediates inorganic nanoparticle assembly by Yi et al. in their comprehensive review.[96]

Innovative trends

Powerful synergy has been realized in the synthesis and templating of inorganic nanoparticles. In this section, we highlight some noteworthy and innovative trends in the area of bottom-up synthesis of nanoparticles as well as additional methods that employ macromolecules. Bachar bioengineered a solar-driven enzyme which will continuously and stereoselectively produce chiral amines, which is a greatly used enantiomer in the pharmaceutical industry.[97] In this study, Cadmium Sulfide (CdS) quantum dots were self-grown onto a protein via CdS-binding peptides that were fused to the structure. The quantum dots acted as a photosensitizer which allowed for efficient and seemingly endless photocatalytic regeneration of a cofactor required in the synthesis of the chiral amine. Additionally, this bioengineered platform for any cofactor-dependent enzymes in the synthesis of fuels and other fine chemicals. There could also be used in utilizing this platform for artificial photosynthesis. A more extensive review regarding bioengineering nano-hybrids can be found by Palomo.[98]

MSA capped CdTe QDs in the presence of poly(diallyldimethylammonium chloride) (PDADMAC) has been shown to undergo self-assembly into luminescent nanodroplets.[99] These droplets have demonstrated selective luminescence quenching only in the presence of Hg^+ ions, allowing for them to be used as ultrasensitive detectors. It was identified that the free carboxylate groups in the MSA capping agent are responsible for the electrostatic attraction of the Hg^+, allowing for the sequestration of these metallic ions. Singh and Mukherjee then utilized this system to act as a reducing agent for AuNPs within the coacervate QD-droplets. [100] By doing so, the peroxidase-activity outperformed that of both QD-droplets and AuNPs individually. The confined AuNPs that formed were well dispersed, 5 nm on average, and stable for a period of at least four weeks. Moreover, the catalytic properties of these coacervate-based catalysts were shown to be recyclable and able to withstand several cycles without loss in performance. The perspective optoelectronic applications that this system could employ is quite large since many different QDs can be capped with a wide variety of capping agents which can be used to tailor to a specific application.

A bioengineering feat was successful by Liu et al. where a fungi was modified to have photocatalytic abilities.[101] CdS nanodots were synthesized intracellularly within the yeast structure allowing for it to become photosensitive and induce enzyme-catalyzed hydrogen production. This can be leveraged for sustainable production of light-driven chemicals like the platform created by Bachar.[97] Additionally, a team led by Kachtík have opted to stray away from organic templates and have deployed an inorganic WS_2 scroll-like nanotube to act as a template for the chiral assembly of metallic, dielectric, and oxide NPs.[102] The advantage of this template is that it is temperature stable to 550C which allows for a wider range of materials to be considered for templating which can allow for advanced applications.

Another innovative application of peptide-mediated NP synthesis is in photothermal therapy. A near-infrared photothermal therapeutic NP was synthesized by Athanasiou et al. with a
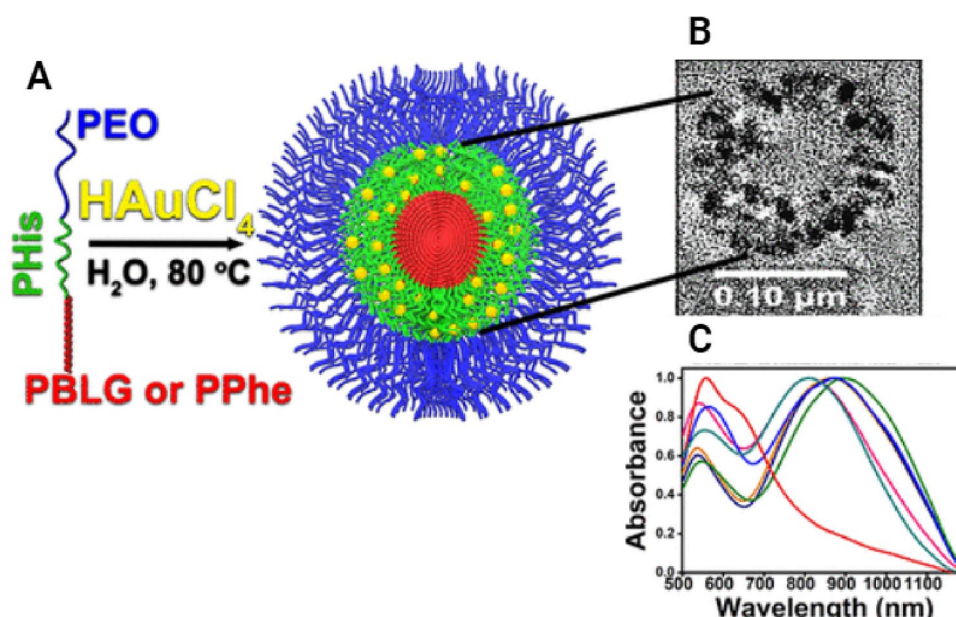
Figure 7. (a) Schematic of the copolypeptide nanoparticle with AuNPs selectively decorating the PHis layer forming the AuNS. (b) TEM images confirming the AuNS with the copolypeptide. (c) UV–VIS measurements demonstrating the ability to control the wavelength selectivity by tuning AuNS size. Adapted from Figs. 1, 2, and 4 in Athanasiou.[28] Copyright © 2021 American Chemical Society.

histidine containing amphiphilic hybrid polypeptide illustrated in Fig. 7(a).[28] These polypeptides formed core–shell self-assemblies that preferentially reduced AuNPs in the histidine layer, as depicted in Fig. 7(b) TEM micrographs, and could vary the size of NP and thickness of Au shell by modifying the peptide molecular characteristics and histidine/Au(III) ratios. Having the ability to change the NP and Au shell size allows for the absorption wavelength to be tuned allowing for the shift to less harmful wavelengths of light making this a safer therapeutic technique which is shown in the UV–VIS measurements as provided in Fig. 7(c).

Future outlook

Inorganic nanoparticles are at the forefront of design spanning from photothermal therapies, targeted drug delivery, specific molecule sensors, and electronics. Top-down methods are unable to offer the same amount of control and diversity that macromolecule-mediated synthesis and templating can. We have reviewed the recent cutting-edge scientific literature that has demonstrated the utility of macromolecule-assisted synthesis and templating of inorganic nanoparticles. Such bottom-up methods have been shown to be compatible with one another, demonstrating the ability to mix different macromolecules and combine benefits from both types for highly specific designs. However, with numerous different macromolecules, the design space is enormous. Therefore, to innovate in this research field, computational design and high-throughput experimentation must be utilized to accelerate and streamline discovery. It is important to emphasize here that many of these macromolecules offer "green synthesis" methods which is important as we address concerns of the twenty first century of pollution and the environment. Overall, innovations in situ synthesis and hierarchal self-assembly of hybrid and multicomponent inorganic NPs by macromolecules can yield smart structures for catalysis, pharmaceuticals, and electronics, making it an exciting and vibrant research field.

Acknowledgments

Author contributions

Brendan Karafinski performed the literature search, data analysis, and drafted the article. Nairiti Sinha had the idea for this article and critically revised the work.

Funding

Data availability

Not applicable.

Declarations
Competing interests

The authors have no competing interests to declare.

References

1. K.M. Mayer, J.H. Hafner, Localized surface plasmon resonance sensors. Chem. Rev. **111**(6), 3828–3857 (2011). https://doi.org/10.1021/cr100313v

2. N. Lee, D.W. Lee, S.M. Lee, Gold nanoparticle-stabilized, tyrosine-rich peptide self-assemblies and their catalytic activities in the reduction of 4-Nitrophenol. Biomacromol **19**(12), 4534–4541 (2018)

3. S. Zhou, M. Maeda, M. Kubo, M. Shimada, One-step synthesis of Gold@ Silica yolk-shell nanoparticles with catalytic activity. Chem. Lett. **50**(8), 1475–1478 (2021). https://doi.org/10.1246/cl.210266

4. P. Li, Y. Wang, H. Huang, S. Ma, H. Yang, Z. Xu, High efficient reduction of 4-Nitrophenol and dye by filtration through Ag NPs coated PAN-Si catalytic membrane. Chemosphere **263**, 127995 (2021). https://doi.org/10.1016/j.chemosphere.2020.127995

5. J. Liu, H. Yu, L. Wang, Effective reduction of 4-Nitrophenol with Au NPs loaded ultrathin two dimensional metal-organic framework nanosheets. Appl. Catal. Gen. **599**, 117605 (2020). https://doi.org/10.1016/j.apcata.2020.117605

6. H. Veisi, Z. Joshani, B. Karmakar, T. Tamoradi, M.M. Heravi, J. Gholami, Ultrasound assisted synthesis of Pd NPs decorated chitosan-starch functionalized Fe_3O_4 nanocomposite catalyst towards Suzuki-Miyaura coupling and reduction of 4-Nitrophenol. Int. J. Biol. Macromol. **172**, 104–113 (2021). https://doi.org/10.1016/j.ijbiomac.2021.01.040

7. T.K. Das, S. Remanan, S. Ghosh, NCh. Das, An environment friendly free-standing cellulose membrane derived for catalytic reduction of 4-nitrophenol: a sustainable approach. J. Environ. Chem. Eng. **9**(1), 104596 (2021). https://doi.org/10.1016/j.jece.2020.104596

8. A.M. Garcia, T.S. Martins, F.F. Camilo, Free facile preparation of Ag-nanoparticles on cellulose membrane for catalysis. Cellulose **28**(8), 4899–4911 (2021). https://doi.org/10.1007/s10570-021-03827-5

9. G.-F. Liu, X.-X. Qiao, Y.-L. Cai, J.-Y. Xu, Y. Yan, B. Karadeniz, J. Lü, R. Cao, Aluminum metal-organic framework–silver nanoparticle composites for catalytic reduction of nitrophenols. ACS Appl. Nano Mater. **3**(11), 11426–11433 (2020). https://doi.org/10.1021/acsanm.0c02516

10. M. Mahani, F. Alimohamadi, M. Torkzadeh-Mahani, Z. Hassani, F. Khakbaz, F. Divsar, M. Yoosefian, LSPR Biosensing for the early-stage prostate cancer detection using hydrogen bonds between PSA and antibody: molecular dynamic and experimental study. J. Mol. Liq. **324**, 114736 (2021). https://doi.org/10.1016/j.molliq.2020.114736

11. J. Tai, S. Fan, S. Ding, L. Ren, Gold nanoparticles based optical biosensors for cancer biomarker proteins: A review of the current practices. Front Bioeng Biotechnol **10**, 877193 (2022)

12. S. Mohammadzadeh-Asl, A. Aghanejad, M. de la Guardia, J.E. Dolatabadi, A. Keshtkar, Surface plasmon resonance signal enhancement based on Erlotinib loaded magnetic nanoparticles for evaluation of its interaction with human lung cancer cells. Optic. Laser Technol. **133**, 106521 (2021)

13. M.H. Jazayeri, T. Aghaie, R. Nedaeinia, M. Manian, H. Nickho, Rapid Non-invasive detection of bladder cancer using survivin antibody-conjugated gold nanoparticles (GNPs) based on localized surface plasmon resonance (LSPR). Cancer Immunol. Immunother. **69**(9), 1833–1840 (2020). https://doi.org/10.1007/s00262-020-02559-y

14. Q. Han, H. Wang, D. Wu, Q. Wei, Preparation of PbS NPs/RGO/NiO nanosheet arrays heterostructure: function-switchable self-powered photoelectrochemical biosensor for H_2O_2 and glucose monitoring. Biosens. Bioelectron. **173**, 112803 (2021). https://doi.org/10.1016/j.bios.2020.112803

15. I. Brice, K. Grundsteins, A. Atvars, J. Alnis, R. Viter, A. Ramanavicius, Whispering gallery mode resonator and glucose oxidase based glucose biosensor. Sens. Actuators B Chem. **318**, 128004 (2020). https://doi.org/10.1016/j.snb.2020.128004

16. G. Emir, Y. Dilgin, A. Ramanaviciene, A. Ramanavicius, Amperometric nonenzymatic glucose biosensor based on graphite rod electrode modified by Ni-Nanoparticle/Polypyrrole composite. Microchem. J. **161**, 105751 (2021). https://doi.org/10.1016/j.microc.2020.105751

17. D. Skrodzki, M. Molinaro, R. Brown, P. Moitra, D. Pan, Synthesis and bioapplication of emerging nanomaterials of hafnium. ACS Nano **18**(2), 1289–1324 (2024). https://doi.org/10.1021/acsnano.3c08917

18. A. Sathiyaseelan, K. Saravanakumar, A.V.A. Mariadoss, M.-H. Wang, pH-Controlled nucleolin targeted release of dual drug from chitosan-gold based aptamer functionalized nano drug delivery system for improved glioblastoma treatment. Carbohydr. Polym. **262**, 117907 (2021). https://doi.org/10.1016/j.carbpol.2021.117907

19. Z. Bian, J. Yan, S. Wang, Y. Li, Y. Guo, B. Ma, H. Guo, Z. Lei, C. Yin, Y. Zhou, M. Liu, K. Tao, P. Hou, W. He, Awakening P53 in Vivo by D-Peptides-functionalized ultra-small nanoparticles: overcoming biological barriers to D-peptide drug delivery. Theranostics **8**(19), 5320–5335 (2018). https://doi.org/10.7150/thno.27165

20. C. Xu, Y. Yan, J. Tan, D. Yang, X. Jia, L. Wang, Y. Xu, S. Cao, S. Sun, Biodegradable nanoparticles of polyacrylic acid-stabilized amorphous CaCO$_3$ for tunable pH-responsive drug delivery and enhanced tumor inhibition. Adv. Funct. Mater. **29**(24), 1808146 (2019). https://doi.org/10.1002/adfm.201808146

21. S.Z. Mat Isa, R. Zainon, M. Tamal, State of the art in gold nanoparticle synthesisation via pulsed laser ablation in liquid and its characterisation for molecular imaging: a review. Materials **15**(3), 875 (2022). https://doi.org/10.3390/ma15030875

22. A.M. Mostafa, E.A. Mwafy, N.S. Awwad, H.A. Ibrahium, Synthesis of multi-walled carbon nanotubes decorated with silver metallic nanoparticles as a catalytic degradable material via pulsed laser ablation in liquid media. Colloids Surf. Physicochem. Eng. Asp. **626**, 126992 (2021). https://doi.org/10.1016/j.colsurfa.2021.126992

23. L.K. Wei, S.Z. Abd Rahim, M.M. Al Bakri Abdullah, A.T. Yin, M.F. Ghazali, M.F. Omar, O. Nemeş, A.V. Sandu, P. Vizureanu, A.E. Abdellah, Producing metal powder from machining chips using ball milling process: a review. Materials **16**(13), 4635 (2023)

24. N. Sakono, Y. Ishida, K. Ogo, N. Tsumori, H. Murayama, M. Sakono, Molar-fraction-tunable synthesis of Ag–Au alloy nanoparticles via a dual evaporation-condensation method as supported catalysts for CO oxidation. ACS Appl. Nano Mater. **6**(4), 3065–3074 (2023). https://doi.org/10.1021/acsanm.3c00089

25. Z. Lin, J. Yue, L. Liang, B. Tang, B. Liu, L. Ren, Y. Li, L. Jiang, Rapid synthesis of metallic and alloy micro/nanoparticles by laser ablation towards water. Appl. Surf. Sci. **504**, 144461 (2020). https://doi.org/10.1016/j.apsusc.2019.144461

26. Y. Xia, J.A. Rogers, K.E. Paul, G.M. Whitesides, Unconventional methods for fabricating and patterning nanostructures. Chem. Rev. **99**(7), 1823–1848 (1999). https://doi.org/10.1021/cr980002q

27. Y. Wen, M.-Q. He, Y.-L. Yu, J.-H. Wang, Biomolecule-mediated chiral nanostructures: a review of chiral mechanism and application. Adv. Colloid Interface Sci. **289**, 102376 (2021). https://doi.org/10.1016/j.cis.2021.102376

28. V. Athanasiou, D. Stavroulaki, Gold nanoparticles and nanoshells embedded as core-shell architectures in hybrid poly(l-Histidine)-containing polymers for photothermal therapies. ACS Appl Nano Mater (2021). https://doi.org/10.1021/acsanm.1c03769

29. B. Muzzi, M. Albino, A. Gabbani, A. Omelyanchik, E. Kozenkova, M. Petrecca, E. Balica, A. Lavacchi, F. Scavone, C. Anceschi, G. Petrucci, A. Ibarra, A. Laurenzana, F. Pineider, V. Rodionova, C. Sangregorio, Star-shaped magnetic-plasmonic Au@Fe3O4 nano-heterostructures for photothermal therapy. ACS Appl. Mater. Interfaces **14**(25), 29087–29098 (2022). https://doi.org/10.1021/acsami.2c04865

30. V.K. LaMer, A.S. Kenyon, Kinetics of the formation of monodispersed sulfur sols from thiosulfate and acid. J. Colloid Sci. **2**(2), 257–264 (1947). https://doi.org/10.1016/0095-8522(47)90026-3

31. K.M.M. Abou El-Nour, A. Eftaiha, A. Al-Warthan, R.A.A. Ammar, Synthesis and applications of silver nanoparticles. Arab. J. Chem. **3**(3), 135–140 (2010). https://doi.org/10.1016/j.arabjc.2010.04.008

32. C. Tojo, F. Barroso, M. de Dios, Critical nucleus size effects on nanoparticle formation in microemulsions: a comparison study between experimental and simulation results. J. Colloid Interface Sci. **296**(2), 591–598 (2006). https://doi.org/10.1016/j.jcis.2005.09.047

33. L. Xu, X. Wang, W. Wang, M. Sun, W.J. Choi, J.-Y. Kim, C. Hao, S. Li, A. Qu, M. Lu, X. Wu, F.M. Colombari, W.R. Gomes, A.L. Blanco, A.F. de Moura, X.

Guo, H. Kuang, N.A. Kotov, C. Xu, Enantiomer-dependent immunological response to chiral nanoparticles. Nature **601**(7893), 366–373 (2022). https://doi.org/10.1038/s41586-021-04243-2

34. A. Yuan, C. Hao, X. Wu, M. Sun, A. Qu, L. Xu, H. Kuang, C. Xu, Chiral CuxOS@ZIF-8 nanostructures for ultrasensitive quantification of hydrogen sulfide In Vivo. Adv. Mater. **32**(19), 1906580 (2020). https://doi.org/10.1002/adma.201906580

35. C. Pigliacelli, R. Sánchez-Fernández, M.D. García, C. Peinador, E. Pazos, Self-assembled peptide–inorganic nanoparticle superstructures: from component design to applications. Chem. Commun. **56**(58), 8000–8014 (2020)

36. Nam, K. T. *Amino-acid- and peptide-directed synthesis of chiral plasmonic gold nanoparticles | Nature.* https://www.nature.com/articles/s41586-018-0034-1 (accessed 2024–01–23).

37. Wang, Y. *Self-Templated, Enantioselective Assembly of an Amyloid-like Dipeptide into Multifunctional Hierarchical Helical Arrays | ACS Nano.* https://pubs.acs.org/doi/full/https://doi.org/10.1021/acsnano.1c00746 (accessed 2024–02–15).

38. J.M. Slocik, P.B. Dennis, A.O. Govorov, N.M. Bedford, Y. Ren, R.R. Naik, Chiral restructuring of peptide enantiomers on gold nanomaterials. ACS Biomater. Sci. Eng. **6**(5), 2612–2620 (2020). https://doi.org/10.1021/acsbiomaterials.9b00933

39. Iu. Mukha, A. Khodko, N. Vityuk, O. Severynovska, V. Pivovarenko, N. Kachalova, N. Smirnova, A. Eremenko, Light-driven formation of gold/tryptophan nanoparticles. Appl. Nanosci. **10**(8), 2827–2833 (2020). https://doi.org/10.1007/s13204-019-01171-6

40. R. Báez-Cruz, L.A. Baptista, S. Ntim, P. Manidurai, S. Espinoza, C. Ramanan, R. Cortes-Huerto, M. Sulpizi, Role of pH in the synthesis and growth of gold nanoparticles using L-asparagine: a combined experimental and simulation study. J. Phys. Condens. Matter **33**(25), 254005 (2021). https://doi.org/10.1088/1361-648x/abf6e3

41. Y. Feng, H. Wang, J. Zhang, Y. Song, M. Meng, J. Mi, H. Yin, L. Liu, Bioinspired synthesis of Au nanostructures templated from amyloid β peptide assembly with enhanced catalytic activity. Biomacromol **19**(7), 2432–2442 (2018). https://doi.org/10.1021/acs.biomac.8b00045

42. P. Chen, G. Wang, C. Hao, W. Ma, L. Xu, H. Kuang, C. Xu, M. Sun, Peptide-directed synthesis of chiral nano-bipyramids for controllable antibacterial application. Chem. Sci. **13**(35), 10281–10290 (2022). https://doi.org/10.1039/D2SC03443C

43. L.D. Pozzo, K.J. Lachowski, K. Vaddi, N.Y. Naser, F. Baneyx, Multivariate analysis of peptide-driven nucleation and growth of Au nanoparticles. Digit. Discov. **1**(4), 427–439 (2022). https://doi.org/10.1039/D2DD00017B

44. A.M. Figat, B. Bartosewicz, M. Liszewska, B. Budner, M. Norek, B.J. Jankiewicz, α-amino acids as reducing and capping agents in gold nanoparticles synthesis using the turkevich method. Langmuir **39**(25), 8646–8657 (2023). https://doi.org/10.1021/acs.langmuir.3c00507

45. B. Briggs, Y. Li, M.T. Swihart, M.R. Knecht, Reductant and sequence effects on the morphology and catalytic activity of peptide-capped Au nanoparticles. ACS Appl. Mater. Interfaces (2015). https://doi.org/10.1021/acsami.5b01461

46. J.I.B. Janairo, Sequence rules for gold-binding peptides. RSC Adv. **13**(31), 21146–21152 (2023). https://doi.org/10.1039/D3RA04269C

47. W. Yang, Q. Yin, C.-L. Chen, Designing sequence-defined peptoids for biomimetic control over inorganic crystallization. Chem. Mater. **33**(9), 3047–3065 (2021). https://doi.org/10.1021/acs.chemmater.1c00243

48. Z. Li, B. Cai, W. Yang, C.-L. Chen, Hierarchical nanomaterials assembled from peptoids and other sequence-defined synthetic polymers. Chem. Rev. **121**(22), 14031–14087 (2021). https://doi.org/10.1021/acs.chemrev.1c00024

49. Chen, C.-L. *Programming Amphiphilic Peptoid Oligomers for Hierarchical Assembly and Inorganic Crystallization | Accounts of Chemical Research.* https://pubs.acs.org/doi/full/https://doi.org/10.1021/acs.accounts.0c00533 (accessed 2024–01–16).

50. N.A. Merrill, F. Yan, H. Jin, P. Mu, C.-L. Chen, M.R. Knecht, Tunable assembly of biomimetic peptoids as templates to control nanostructure catalytic activity. Nanoscale **10**(26), 12445–12452 (2018). https://doi.org/10.1039/c8nr03852j

51. M. Monahan, B. Cai, T. Jian, S. Zhang, G. Zhu, C.L. Chen, J.J. De Yoreo, B.M. Cossairt, Peptoid-directed assembly of CdSe nanoparticles. Nanoscale **13**(2), 1273–1282 (2021)

52. F. Yan, L. Liu, T.R. Walsh, Y. Gong, P.Z. El-Khoury, Y. Zhang, Z. Zhu, J.J. De Yoreo, M.H. Engelhard, X. Zhang, C.-L. Chen, Controlled synthesis of highly-branched plasmonic gold nanoparticles through peptoid engineering. Nat. Commun. **9**(1), 2327 (2018). https://doi.org/10.1038/s41467-018-04789-2

53. W. Yang, Y. Zhou, B. Jin, X. Qi, B. Cai, Q. Yin, J. Pfaendtner, J.J. De Yoreo, C.-L. Chen, Designing sequence-defined peptoids for fibrillar self-assembly and silicification. J. Coll. Interface Sci. **634**, 450–459 (2023). https://doi.org/10.1016/j.jcis.2022.11.136

54. B. Jin, F. Yan, X. Qi, B. Cai, J. Tao, X. Fu, S. Tan, P. Zhang, J. Pfaendtner, N.Y. Naser, F. Baneyx, X. Zhang, J.J. DeYoreo, C.-L. Chen, Peptoid-directed formation of five-fold twinned Au nanostars through particle attachment and facet stabilization. Angew. Chem. **134**(14), e202201980 (2022). https://doi.org/10.1002/ange.202201980

55. J. Ma, B. Jin, K.N. Guye, Md.E. Chowdhury, N.Y. Naser, C.-L. Chen, J.J. De Yoreo, F. Baneyx, Controlling mineralization with protein-functionalized peptoid nanotubes. Adv. Mater. **35**(3), 2207543 (2023). https://doi.org/10.1002/adma.202207543

56. Y. Shang, N. Li, S. Liu, L. Wang, Z.-G. Wang, Z. Zhang, B. Ding, Site-specific synthesis of silica nanostructures on DNA origami templates. Adv. Mater. **32**(21), 2000294 (2020). https://doi.org/10.1002/adma.202000294

57. J. Yesuraj, S. Austin Suthanthiraraj, O. Padmaraj, Synthesis, characterization and electrochemical performance of DNA-templated Bi_2MoO_6 nanoplates for supercapacitor applications. Mater. Sci. Semicond. Process. **90**, 225–235 (2019). https://doi.org/10.1016/j.mssp.2018.10.030

58. K. Morikawa, Y. Masubuchi, Y. Shchipunov, A. Zinchenko, DNA-Chitosan hydrogels: formation, properties, and functionalization with catalytic nanoparticles. ACS Appl. Bio Mater. **4**(2), 1823–1832 (2021). https://doi.org/10.1021/acsabm.0c01533

59. D. Mathur, W.P. Klein, M. Chiriboga, H. Bui, E. Oh, R. Nita, J. Naciri, P. Johns, J. Fontana, S.A. Díaz, I.L. Medintz, Analyzing fidelity and reproducibility of DNA templated plasmonic nanostructures. Nanoscale **11**(43), 20693–20706 (2019)

60. Y. Liu, L. Ma, S. Jiang, C. Han, P. Tang, H. Yang, X. Duan, N. Liu, H. Yan, X. Lan, DNA programmable self-assembly of planar, thin-layered chiral nanoparticle superstructures with complex two-dimensional patterns. ACS Nano **15**(10), 16664–16672 (2021). https://doi.org/10.1021/acsnano.1c06639

61. S. Wang, P.-A. Lin, M. DeLuca, S. Zauscher, G. Arya, Y. Ke, Controlling silicification on DNA origami with polynucleotide brushes. J. Am. Chem. Soc. **146**(1), 358–367 (2024). https://doi.org/10.1021/jacs.3c09310

62. P. Zhao, B. Li, Y. Li, L. Chen, H. Wang, L. Ye, DNA-templated ultrasmall bismuth sulfide nanoparticles for photoacoustic imaging of myocardial infarction. J. Coll. Interface Sci. **615**, 475–484 (2022). https://doi.org/10.1016/j.jcis.2022.01.194

63. H. Zhao, J. Lv, F. Li, Z. Zhang, C. Zhang, Z. Gu, D. Yang, Enzymatical biomineralization of DNA nanoflowers mediated by manganese ions for tumor site activated magnetic resonance imaging. Biomaterials **268**, 120591 (2021). https://doi.org/10.1016/j.biomaterials.2020.120591

64. H. Fang, X. Zhang, D. Gao, Y. Xiao, L. Ma, H. Yang, Y. Zhou, Fluorescence determination of glyphosate based on a DNA-templated copper nanoparticle biosensor. Microchim. Acta **189**(4), 158 (2022). https://doi.org/10.1007/s00604-022-05284-8

65. M. Stanisz, Ł. Klapiszewski, T. Jesionowski, Recent advances in the fabrication and application of biopolymer-based micro- and nanostructures: a comprehensive review. Chem. Eng. J. **397**, 125409 (2020). https://doi.org/10.1016/j.cej.2020.125409

66. Keating, C. D. 2023 *Bioinspired Mineralizing Microenvironments Generated by Liquid-Liquid Phase Coexistence*; DOE-PSU-1; Pennsylvania State Univ., University Park, PA (United States). https://doi.org/10.2172/1843375.

67. K. Li, Y. Li, X. Wang, M. Cui, B. An, J. Pu, J. Liu, B. Zhang, G. Ma, C. Zhong, Diatom-inspired multiscale mineralization of patterned protein-polysaccharide complex structures. Natl. Sci. Rev. (2021). https://doi.org/10.1093/nsr/nwaa191

68. Z. Sabouri, S.S. Moghaddas, A. Mostafapour, M. Darroudi, Biopolymer-template synthesized $CaSO_4$ nanoparticles and evaluation of their photocatalytic activity and cytotoxicity effects. Ceram. Int. **48**(11), 16306–16311 (2022)

69. A. Scala, A. Piperno, A. Hada, S. Astilean, A. Vulpoi, G. Ginestra, A. Marino, A. Nostro, V. Zammuto, C. Gugliandolo, Marine bacterial exopolymers-mediated green synthesis of noble metal nanoparticles with antimicrobial properties. Polymers **11**(7), 1157 (2019). https://doi.org/10.3390/polym11071157

70. L. Martinaga, R. Ludwig, I. Rezić, M. Andlar, D. Pum, A. Vrsalović Presečki, The application of bacteria-derived dehydrogenases and oxidases in the synthesis of gold nanoparticles. Appl. Microbiol. Biotechnol. **108**(1), 62 (2024). https://doi.org/10.1007/s00253-023-12853-1

71. L. Lv, X. Wu, Y. Yang, X. Han, R. Mezzenga, C. Li, Trans-scale 2D synthesis of millimeter-large Au single crystals via silk fibroin templates. ACS Sustain. Chem. Eng. **6**(9), 12419–12425 (2018). https://doi.org/10.1021/acssuschemeng.8b02954

72. H. Tohidi, N. Maleki-Jirsaraei, A. Simchi, F. Mohandes, Z. Emami, L. Fassina, F. Naro, B. Conti, F. Barbagallo, An electroconductive, thermosensitive, and injectable chitosan/pluronic/gold-decorated cellulose nanofiber hydrogel as an efficient carrier for regeneration of cardiac tissue. Materials **15**(15), 5122 (2022). https://doi.org/10.3390/ma15155122

73. A.S. Doghish, A.H. Hashem, A.M. Shehabeldine, A.-A.M. Sallam, G.S. El-Sayyad, S.S. Salem, Nanocomposite based on gold nanoparticles and carboxymethyl cellulose: synthesis, characterization, antimicrobial, and anticancer activities. J. Drug Deliv. Sci. Technol. **77**, 103874 (2022). https://doi.org/10.1016/j.jddst.2022.103874

74. M. Alle, S.C. Park, R. Bandi, S.-H. Lee, J.-C. Kim, Rapid In-Situ growth of gold nanoparticles on cationic cellulose nanofibrils: recyclable nanozyme for the colorimetric glucose detection. Carbohydr. Polym. **253**, 117239 (2021). https://doi.org/10.1016/j.carbpol.2020.117239

75. Md.K. Haider, A. Ullah, M.N. Sarwar, Y. Saito, L. Sun, S. Park, I.S. Kim, Lignin-mediated in-Situ synthesis of CuO nanoparticles on cellulose nanofibers: a potential wound dressing material. Int. J. Biol. Macromol. **173**, 315–326 (2021). https://doi.org/10.1016/j.ijbiomac.2021.01.050

76. L. Valencia, S. Kumar, E.M. Nomena, G. Salazar-Alvarez, A.P. Mathew, In-Situ growth of metal oxide nanoparticles on cellulose nanofibrils for dye removal and antimicrobial applications. ACS Appl. Nano Mater. **3**(7), 7172–7181 (2020). https://doi.org/10.1021/acsanm.0c01511

77. S.M. Albukhari, M. Ismail, K. Akhtar, E.Y. Danish, Catalytic reduction of nitrophenols and dyes using silver nanoparticles @ cellulose polymer paper for the resolution of waste water treatment challenges. Colloids Surf. Physicochem. Eng. Asp. **577**, 548–561 (2019). https://doi.org/10.1016/j.colsurfa.2019.05.058

78. A. Hassan, N.M. Sorour, A. El-Baz, Y. Shetaia, Simple synthesis of bacterial cellulose/magnetite nanoparticles composite for the removal of antimony from aqueous solution. Int. J. Environ. Sci. Technol. **16**(3), 1433–1448 (2019). https://doi.org/10.1007/s13762-018-1737-4

79. H.B. Ahmed, M.A. Attia, F.M.S.E. El-Dars, H.E. Emam, Hydroxyethyl cellulose for spontaneous synthesis of antipathogenic nanostructures: (Ag & Au) nanoparticles versus Ag-Au nano-alloy. Int. J. Biol. Macromol. **128**, 214–229 (2019). https://doi.org/10.1016/j.ijbiomac.2019.01.093

80. Z. Yu, C. Hu, L. Guan, W. Zhang, J. Gu, Green synthesis of cellulose nanofibrils decorated with Ag nanoparticles and their application in colorimetric detection of L-Cysteine. ACS Sustain. Chem. Eng. **8**(33), 12713–12721 (2020). https://doi.org/10.1021/acssuschemeng.0c04842

81. Kim, M. *Block Copolymer Enabled Synthesis and Assembly of Chiral Metal Oxide Nanoparticle | ACS Nano*. https://pubs.acs.org/doi/full/https://doi.org/10.1021/acsnano.3c00047 (accessed 2024–02–15).

82. I. Weisbord, N. Shomrat, H. Moshe, A. Sosnik, T. Segal-Peretz, Nano spray-dried block copolymer nanoparticles and their transformation into hybrid and inorganic nanoparticles. Adv. Funct. Mater. **30**(18), 1808932 (2020). https://doi.org/10.1002/adfm.201808932

83. J. Zhou, C. Zhang, Y. Wang, Nanoporous block copolymer membranes immobilized with gold nanoparticles for continuous flow catalysis. Polym. Chem. **10**(13), 1642–1649 (2019). https://doi.org/10.1039/C8PY01789A

84. T. Kim, M. Xu, Y.J. Lee, K.H. Ku, D.J. Shin, D.C. Lee, S.G. Jang, H. Yun, B.J. Kim, Fluorescence switchable block copolymer particles with doubly alternate-layered nanoparticle arrays. Small **17**(28), 2101222 (2021). https://doi.org/10.1002/smll.202101222

85. K. Jia, J. Xie, X. He, D. Zhang, B. Hou, X. Li, X. Zhou, Y. Hong, X. Liu, Polymeric micro-reactors mediated synthesis and assembly of Ag nanoparticles into cube-like superparticles for SERS application. Chem. Eng. J. **395**, 125123 (2020). https://doi.org/10.1016/j.cej.2020.125123

86. M. Alle, T.H. Kim, S.H. Park, S.H. Lee, J.C. Kim, Doxorubicin-carboxymethyl xanthan gum capped gold nanoparticles: microwave synthesis, characterization, and anti-cancer activity. Carbohydr. Polym. **229**, 115511 (2020)

87. A. Rai, S. Bhaskar, S.S. Ramamurthy, Plasmon-coupled directional emission from soluplus-mediated AgAu nanoparticles for Attomolar sensing using a smartphone. ACS Appl. Nano Mater. **4**(6), 5940–5953 (2021). https://doi.org/10.1021/acsanm.1c00841

88. X. He, L. Dai, L. Ye, X. Sun, O. Enoch, R. Hu, X. Zan, F. Lin, J. Shen, A vehicle-free antimicrobial polymer hybrid gold nanoparticle as synergistically therapeutic platforms for staphylococcus aureus infected wound healing. Adv. Sci. **9**(14), 2105223 (2022). https://doi.org/10.1002/advs.202105223

89. P. Liu, J. Peng, Y. Chen, M. Liu, W. Tang, Z.-H. Guo, K. Yue, A general and robust strategy for in-Situ templated synthesis of patterned inorganic nanoparticle assemblies. Giant **8**, 100076 (2021). https://doi.org/10.1016/j.giant.2021.100076

90. W.-L. Wang, A. Kanno, A. Ishiguri, R.-H. Jin, Generation of Sub-5 Nm AuNPs in the special space of the loop-cluster corona of a polymer vesicle: preparation and its unique catalytic performance in the reduction of 4-nitrophenol. Nanoscale Adv. **5**(8), 2199–2209 (2023). https://doi.org/10.1039/D2NA00893A

91. L.P. Bressan, J. Robles-Najar, C.B. Adamo, R.F. Quero, B.M.C. Costa, D.P. de Jesus, J.A.F. da Silva, 3D-printed microfluidic device for the synthesis of silver and gold nanoparticles. Microchem. J. **146**, 1083–1089 (2019). https://doi.org/10.1016/j.microc.2019.02.043

92. L. Kool, A. Bunschoten, A.H. Velders, V. Saggiomo, Gold nanoparticles embedded in a polymer as a 3D-printable dichroic nanocomposite material. Beilstein J. Nanotechnol. **10**(1), 442–447 (2019). https://doi.org/10.3762/bjnano.10.43

93. T. Valayil Varghese, J. Eixenberger, F. Rajabi-Kouchi, M. Lazouskaya, C. Francis, H. Burgoyne, K. Wada, H. Subbaraman, D. Estrada, Multijet gold nanoparticle inks for additive manufacturing of printed and wearable electronics. ACS Mater. Au **4**(1), 65–73 (2024). https://doi.org/10.1021/acsmaterialsau.3c00058

94. B. Begines, A. Alcudia, R. Aguilera-Velazquez, G. Martinez, Y. He, G.F. Trindade, R. Wildman, M.-J. Sayagues, A. Jimenez-Ruiz, R. Prado-Gotor, Design of highly stabilized nanocomposite inks based on biodegradable polymer-matrix and gold nanoparticles for inkjet printing. Sci. Rep. **9**(1), 16097 (2019). https://doi.org/10.1038/s41598-019-52314-2

95. P.A. Loughney, K.L. Martin, P. Cuillier, E.B. Trigg, N.D. Posey, M.B. Dickerson, T.L. Pruyn, V. Doan-Nguyen, Pre-ceramic polymer-assisted nucleation and growth of copper sulfide nanoplates. Commun. Mater. **4**(1), 1–8 (2023). https://doi.org/10.1038/s43246-023-00380-5

96. C. Yi, Y. Yang, B. Liu, J. He, Z. Nie, Polymer-guided assembly of inorganic nanoparticles. Chem. Soc. Rev. **49**(2), 465–508 (2020). https://doi.org/10.1039/C9CS00725C

97. O. Bachar, M.M. Meirovich, Y. Zeibaq, O. Yehezkeli, Protein-mediated biosynthesis of semiconductor nanocrystals for photocatalytic NAD(P)H regeneration and chiral amine production. Angew. Chem. Int. Ed. **61**(23), e202202457 (2022). https://doi.org/10.1002/anie.202202457

98. M. Palomo, J. Nanobiohybrids, A new concept for metal nanoparticles synthesis. Chem. Commun. **55**(65), 9583–9589 (2019). https://doi.org/10.1039/C9CC04944D

99. S. Singh, J.K. Vaishnav, T.K. Mukherjee, Quantum dot-based hybrid coacervate nanodroplets for ultrasensitive detection of Hg2+. ACS Appl. Nano Mater. **3**(4), 3604–3612 (2020). https://doi.org/10.1021/acsanm.0c00317

100. S. Singh, T.K. Mukherjee, Coacervate-based plexcitonic assembly toward peroxidase-like activity and ultrasensitive glucose sensing. ACS Appl. Mater. Interfaces **15**(21), 25524–25535 (2023). https://doi.org/10.1021/acsami.3c02863

101. P. Liu, Y. Chang, X. Ren, T. Liu, H. Meng, X. Ru, Z. Bai, L. Yang, X. Ma, Endowing cells with unnatural photocatalytic ability for sustainable chemicals production by bionic minerals-triggering. Green Chem. **25**(1), 431–438 (2023). https://doi.org/10.1039/D2GC03534K

102. L. Kachtik, D. Citterberg, K. Bukvišová, L. Kejík, F. Ligmajer, M. Kovařík, T. Musálek, M. Krishnappa, T. Šikola, M. Kolíbal, Chiral nanoparticle chains on inorganic nanotube templates. Nano Lett. **23**(13), 6010–6017 (2023). https://doi.org/10.1021/acs.nanolett.3c01213